Revisiting Concrete Spall and Breach Prediction Curves: Strain Rate (Scale Effect) and Impulse (Pulse Length and Charge Shape) Considerations

by:

Kirk A. Marchand, SwRI
Stan Woodson, USAWES
Tim Knight, USACE/Omaha

ABSTRACT

Prediction of concrete structure spall and breach as generated by tactical weapons ranging in size from small mortars up to large aircraft bombs in size has traditionally been accomplished through the use of empirically generated prediction curves and algorithms based on data fits to those curves. Past attempts in generating these curves have resulted in less than satisfactory results when scaled thickness ($T/W^{1/3}$) and scaled distance ($R/W^{1/3}$) only were considered. Even when "correction factors" for casing were applied, the data scatter was significant. Work done to consider additional physical parameters important to this localized concrete response is described in this paper. Parameters allowing for the consideration of casing thickness, strain rate effect on strength associated with scale size of experiments, and cylindrical charge shape effects on impulse have been included in the analysis.

The work reported herein was directly funded by Dr. Stan Woodson of the US Army Waterways Experiment Station in Vicksburg, Mississippi. Mr. Tim Knight of the Omaha District served with Dr. Woodson as a technical monitor. The analysis was conducted at the Southwest Research Institute in San Antonio, Texas, USA.

Introduction - Previous work done to define the threshold thicknesses for concrete spall and breach (References 1 and 2) has presented the data in parameters consisting of the terms T (thickness), R (standoff), W (charge weight), and W_c (case weight). Analysis of the data using only these parameters creates several problems. One important but neglected factor is the strain rate effect on concrete strength. It has been observed in numerous tests over the years that localized response of concrete structures, particularly spall and breach, is not well predicted using replica modelling laws of engineering dynamics. In other words the linear geometric and volumetric damage cannot be well predicted by the scale factor $(\text{length})^2$ or $(\text{length})^3$. Increases in apparent concrete strength (dominated by compressive increases at very small or contact standoffs, and tensile increases at larger standoffs) are shown in this paper to allow better data comparisons between prototype and subscale tests.

Secondly, past analyses have not explicitly incorporated blast impulse into the analysis. Impulse is important for two reasons: first, breach is certainly very dependant on the time

Report Documentation Page

Form Approved
OMB No. 0704-0188

Public reporting burden for the collection of information is estimated to average 1 hour per response, including the time for reviewing instructions, searching existing data sources, gathering and maintaining the data needed, and completing and reviewing the collection of information. Send comments regarding this burden estimate or any other aspect of this collection of information, including suggestions for reducing this burden, to Washington Headquarters Services, Directorate for Information Operations and Reports, 1215 Jefferson Davis Highway, Suite 1204, Arlington VA 22202-4302. Respondents should be aware that notwithstanding any other provision of law, no person shall be subject to a penalty for failing to comply with a collection of information if it does not display a currently valid OMB control number.

1. REPORT DATE	2. REPORT TYPE	3. DATES COVERED
AUG 1994		**00-00-1994 to 00-00-1994**

4. TITLE AND SUBTITLE	5a. CONTRACT NUMBER
Revisiting Concrete Spall and Breach Prediction Curves: Strain Rate (Scale Effect) and Impulse (Pulse Length and Charge Shape) Considerations	5b. GRANT NUMBER
	5c. PROGRAM ELEMENT NUMBER
6. AUTHOR(S)	5d. PROJECT NUMBER
	5e. TASK NUMBER
	5f. WORK UNIT NUMBER
7. PERFORMING ORGANIZATION NAME(S) AND ADDRESS(ES) **Army Engineer Waterways Experiment Station,ATTN: CEWES-SS-R,3909 Halls Ferry Road,Vicksburg,MS,39180-6199**	8. PERFORMING ORGANIZATION REPORT NUMBER
9. SPONSORING/MONITORING AGENCY NAME(S) AND ADDRESS(ES)	10. SPONSOR/MONITOR'S ACRONYM(S)
	11. SPONSOR/MONITOR'S REPORT NUMBER(S)

12. DISTRIBUTION/AVAILABILITY STATEMENT
Approved for public release; distribution unlimited

13. SUPPLEMENTARY NOTES
See also ADM000767. Proceedings of the Twenty-Sixth DoD Explosives Safety Seminar Held in Miami, FL on 16-18 August 1994.

14. ABSTRACT
see report

15. SUBJECT TERMS

16. SECURITY CLASSIFICATION OF:			17. LIMITATION OF ABSTRACT	18. NUMBER OF PAGES	19a. NAME OF RESPONSIBLE PERSON
a. REPORT	b. ABSTRACT	c. THIS PAGE			
unclassified	**unclassified**	**unclassified**	**Same as Report (SAR)**	**25**	

integral of pressure, and second, the mechanism whereby the "trapped" reflected tensile impulse generates spall is dependant upon the shape of the stress wave caused by the applied pressure history after it has propagated into the concrete.

Finally the analysis reported here has incorporated the charge shape or charge aspect ratio effects on applied impulse for close-in loadings ($R/W^{1/3}<2.0$). This adjustment is significant for the many experiments that have been accomplished with cylindrical explosive charges.

Similitude Analysis - A complete review of all of the pertinent parameters for spall and breach prediction was accomplished and a similitude analysis was performed. The parameters considered included:

pulse duration (d),
reflected pressure (P_r) - to account for force effects,
standoff (R),
charge weight (W),
concrete strength (f'_C) - including a dynamic increase factor as a function of strain rate, to account for scale effects,
concrete thickness (T),
spall diameter (D_S),
breach diameter (D_b),
rebar spacing (s),
reinforcement ratio (p),
reflected impulse (i), and
case weight (Wc).

Also, scaled terms for use in a data analysis were postulated, and data analysis of some 400 spall and breach test data points was performed.

The pi terms developed and used in the similitude analysis are presented below. These are scale independent terms which are intended to normalize parameters from different scaled tests into comparable terms:

EQUATIONS

Scaled Pressure $$\frac{P}{f'_c}$$

Scaled Standoff $$\frac{R f'^{1/3}_c}{W^{1/3}}$$

Scaled Thickness $$\frac{T}{R}$$

Scaled Specific Impulse $$\frac{i}{f'_c d}$$

Scaled Case Weight Ratio $$\frac{W}{W + W_c}$$

Spall and breach diameter analyses were also investigated early in this effort, but it was decided that the main task effort should be applied to spall and breach threshold analysis.

The charge weight W has been modified in the scaled standoff term and in the scaled case weight ratio term to include aspect ratio (cylindrical vs spherical charge geometry) effects. Charge weight is first modified in the analysis by calculating an impulse increase factor based on the ratio of presented area of the cylindrical charge versus the presented area of an equivalent weight spherical charge. This effect is then decayed from a maximum multiplier on impulse at 0 standoff to negligible effect on impulse at a scaled standoff ($R/W^{1/3}$) of 2.0. A new or equivalent charge weight is then calculated through a cubic solution of the Kingery equation for impulse. This is simplified in the analysis by the observation that, for close-in standoffs, percentage of charge weight increase is twice that of the impulse increase.

The resulting equation for the calculation of charge weight increase at scaled standoffs less than 2.0 for cylindrical charges is as follows (L and D are the length and diameter respectively of the cylindrical charge):

EQUATION

$$W_{adj} = W\left\{2\left\{LD/\left[\pi\left(\frac{3LD^2}{16}\right)^{2/3}\right]-1\right\}\left\{1-\frac{R}{2W^{1/3}}\right\}+1\right\}$$

Case weight is included in the analysis by multiplying the scaled standoff term by the scaled case weight ratio term. The selection of the 1/3 power in the scaled case weight ratio term was done somewhat by observation, but indeed seems to make sense since the charge weight in the scaled term is raised to that same power. Additionally, the shift in the data is reasonable based on the shift of the unaltered "McVay" (Reference 1) data as illustrated later in this report.

Strain rate effects (scale effects) are included in the analysis by multiplying the concrete strength, f'_c by a dynamic increase factor or DIF based on strain rate. The DIF is calculated as follows:

EQUATION

$$DIF_{tensile} = \dot{\varepsilon}^{\left(\frac{1}{2.5}\right)} \quad ; \quad DIF_{compressive} = \dot{\varepsilon}^{\left(\frac{1}{6.7}\right)}$$

where:

$$\dot{\varepsilon} = \frac{\dot{P}}{E_{concrete}}$$

$$\dot{P} = \frac{P_r^2}{2(i_r)}$$

These relationships for DIF (ratio of dynamic to static strength) are based on work by Ross at Tyndall AFB (Reference 3).

Data Analysis - The modified equations were applied to a data set derived from tests at SwRI (References 4 and 5), the McVay data set (Reference 1), and the Eglin "Amend" data sets (References 6 and 7). The "no damage/spall/breach" parameters were used to perform the threshold analysis. It should be noted that the Eglin and SwRl data sets were adjusted by multiplying the SwRI charge weights by 0.5 to account for "free air" conditions, and the Eglin charge weights by 2.0 to account for reflections inside the test chamber used in those tests. Other data subsets, originally used by McVay in his analysis, were evaluated and sometimes removed from the database due to undefined or unusual charge geometries, unusual material properties (fiber concrete), unusual test conditions (duplicate tests on a damaged concrete wall), or undefined case properties and weights. **It is important to note that all of the data reported herein is presented in a form assuming hem is pherical surface bursts and the design curves are presented for hem is pherical surface burst cases.**

The final product of this analysis will certainly be similar to that found in existing references. The following sequence of plots, ultimately ending with our recommended design plot, presents data sets using the scaled terms as defined by others and finally as proposed here. It should be noted that the units used for all plots are feet, pounds, and pounds per square inch for strength.

Figure 1 presents the spall and breach data from McVay. This figure shows the format of the most recent compilations of spall and breach data. The second plot in the series (Figure 2) shows the compilation and scaling of spall data as presented in ARA Report 5555 (Reference 2), where a sophisticated statistical analysis was used in an attempt to develop better guidance for designing against spall. As shown in that plot, the recommended curve underpredicts scaled thickness particularly as their scaled standoff approaches 1.0. The third plot in the series, Figure 3, presents spall and breach data, using the scaled R from McVay, and the scaled T as T/R. This plot presents the same data set shown in Figure 1 with McVay's scaled standoff term, but with the proposed scaled thickness term, T/R. Comparing Figures 1 and 3 it can be seen that a better grouping of the spall data is achieved, probably because the thickness is scaled simply as a function of standoff, not charge size. This implies that the pressure term is probably more important than the impulse term for thickness required to prevent spall since pressure, according to Hopkinson scaling is a direct function of scaled standoff. Figure 4 shows the next step, which is to scale the case weight adjustment term by the cube root. This brings the no damage, spall and breach data for cased weapons into a tighter band.

Finally, Figures 5 and 6 are presented, which show the recommended data and scaling approach. (Figure 6 simply shows the full range of the data studied.) Here the same T/R term is used to scale thickness, and strength is added into the scaled standoff term (one DlF is used for contact explosions assuming that compressive strength controls, the other strength increase is used for non-contact explosions where tensile strength is assumed to control). The strength terms were added in the scaled standoff term by expressing the required dynamic increase factor or DIF as a function of R, f'c and W as follows.

First P_r and I_r were determined from simple fits to the reflected airblast parameters at close-in standoffs and are defined as:

EQUATIONS

$$P_r = \frac{W^{.399}}{R^{1.2}} (8000) \qquad i_r = \frac{W^{.949}}{R^{1.85}} (250)$$

Then,

$$DIF = \left[\frac{P_r^2}{2 i_r E_{conc}}\right]^K$$

where $E_{conc} = 57{,}000 (f'_c)^{1/2}$, and K = 0.15 for contact charges when $DIF_{compressive}$ controls, and K = 0.4 for non-contact charges when $DIF_{tension}$ controls.

$$DIF_{contact} = \left[\frac{8000^2 \; 1000 (W^{.379})^2 R^{1.85}}{2(250)(57{,}000) f'^{.5}_c W^{.949} (R^{1.2})^2}\right]^{.15}$$

$$= 3.18 \; W^{-.023} R^{-.083} f'^{-.075}_c$$

$$DIF_{close\text{-}in} = \left[\frac{8000^2 \; 1000 (W^{.379})^2 R^{1.85}}{2(250)(57{,}000) f'^{.5}_c W^{.949} (R^{1.2})^2}\right]^{.4}$$

$$= 21.9 \; W^{-.060} \; R^{-.220} \; f'^{-.20}_c$$

The scaled standoff terms were then developed as described below:

EQUATIONS

$$\text{Scaled standoff}_{\text{contact}} = R f'_c{}^{1/3} / W^{1/3}$$

$$= \frac{R\,(3.18\,W^{-.023}\,R^{-.083}\,f'_c{}^{-.075}\,f'_c)^{1/3}}{W^{1/3}}$$

$$= .527\,R^{.972}\,f'_c{}^{.308}\,W^{-.341}$$

$$\text{Scaled standoff}_{\text{close-in}} = \frac{R\,(21.9\,W^{-.060}\,R^{-.220}\,f'_c{}^{-.20})^{1/3}}{W^{1/3}} \left(\frac{W}{W+W_c}\right)^{1/3}$$

$$= R^{.926}\,f'_c{}^{.266}\,W^{-.353} \left(\frac{W}{W+W_c}\right)^{1/3}$$

$$\text{Scaled Thickness} = \frac{T}{R}$$

It should be noted that the close-in term was normalized by an equation constant, as was the contact term.

Next, fits to the upper range of the spall and breach data sets were required for design guidance. The threshold "fits" presented on the attached plot as Figure 7 were generated "by eye" and are described by the following equations:

EQUATIONS

Spall Fit: $$y = \frac{1}{a + bx^{2.5} + cx^{0.5}} \quad \begin{cases} a = -.02511 \\ b = .01004 \\ c = .13613 \end{cases}$$

Breach Fit: $$y = \frac{1}{a + bx + cx^{2}} \quad \begin{cases} a = .028205 \\ b = .144308 \\ c = .049265 \end{cases}$$

Figures 8 and 9, then, show the 95% prediction interval for spall; Figure 8 contains all of the data, and Figure 9 shows just spall data.

The limits of applicability of the curves are stated below as the limits and averages of the data used in the analysis:

TABLE 1

Parameter	Max.	Min.	Avg.
R, in.	360	0.1	21.0
W, lb.	2299	0.03	24.4
Length, in.	60.0	0.80	8.8
Dia., in.	18.0	0.80	4.0
Case Thick., in.	0.62	0.00	0.05
$R/W^{1/3}$, $in/lb^{1/3}$	12.1	0.008	0.70
T, in.	84.0	2.00	9.23
f'_c, psi	13815	1535	5067
S, in.	11.8	1.25	7.16
ρ	0.025	0.0005	0.0054

Data comparisons - In order to demonstrate improvements which the proposed data presentation provides over previous attempts and to illustrate the effects of test or charge scale, case weight and charge shape or aspect ratio, several pairs of data comparisons are presented on Figures 10 - 13.

Figure 10 illustrates how the effect of scale is accounted for using the new curves. McVay's tests 1A and 2D were 1/3 scale models of full scale tests Box 10 and Box 7, respectively. As shown in the plot, the small scale models should be damaged less than their corresponding full scale structures. McVay's data proves this, which suggests that the rate effect factor applied to scaled standoff does adjust the data appropriately.

Figures 11 and 12 present the results of several of McVay's tests of bare and cased charges of the same explosive weight. Bare charge results from tests 1 C, 1 A, 2B, Box 1, Box 4, and Box 8 may be compared with cased charge tests 2C, 1 B, 2D, Box 2, Box 5, and Box 9, respectively. (Tests 1C and 2C are presented on Figure 12.) The casing effect is readily observed and is reasonably well predicted at larger scaled standoffs; Figure 12 suggests that, at smaller scaled standoffs, the casing effect has little significance.

Figure 13 illustrates the effect of charge shape on damage. Results from tests by Vargas (References 4 and 5) at SwRI demonstrate this effect. Test pairs 1/2, 3/4, 5/6, and 7/8 were of equal charge weight and standoff against the same target, but charges 2, 4, 6, and 7 were spheres; charges 1, 3, 5, and 8 were L/D=4 cylinders.

Recommendations for Future Work - Finally, the scope of this project did not permit revisiting all of the spall and breach data available and referenced in the literature. Additionally, while spall and breach diameter analysis was initiated, sufficient time and budget were not available to complete that task.

We recommend that additional work be undertaken to further investigate and refine this database. We also recommend that further analysis be undertaken to improve the spall diameter analysis, and breach diameter analysis, and, to add a spall depth and breach volume analysis so as to allow these important parameters to be presented as simply as the threshold analysis has been presented herein. A further benefit of the depth and volume analysis will be the prediction of failed masses, certainly important in vulnerability and Iethality studies.

REFERENCES

1. McVay, Mark K., "Spaii Damage of Concrete Structures," Technical Report SL 88-22, US Army Waterways Experiment Station, Vicksburg, Mississippi, June 1988.

2. Twisdale, L.A., Sues, R.H. and Lavelle, "Reliability Based Analysis and Design Methods for Reinforced Concrete Protective Structures," Applied Research Associates Report No. 5555, Air Force Civil Engineering Support Agency, Tyndal AFB, FL, August 1992.

3. Ross, C.A., Kuennen, S.T., and Tedesco, J.W., "Effects of Strain-Rate on Concrete Strength," Presented at the American Concrete Institute Spring Convention, March 1992.

4. Marchand, K.A., Vargas, L.M., and Nixon, J.D., "The Synergistic Effects of Combined Blast and Fragment Loadings," Air Force Engineering and Services Center report ESL-TR-91-18, Tyndall AFB, FL, January 1992.

5. Vargas, L.M., Esparza, E.D., Marchand, K.A., and Bowles, P.k., "Additional Tests to Support rewrite of DOE/TIC-I 1268: A Manual for the Prediction of Blast and Fragment Loadings on Structures," SwRI Project Report No. 06-4279, Contract No. H95 1 4600/FFPOO3542, September 1993.

6. Brown, L., Wisotski, J., and Lynch, R., "Blast/Fragment Effects from Cased and Uncased Charges," AFATL Report AFATL-TR-89-84, Denver Research Institute, January 1990.

7. Preliminary data from tests conducted at Eglin AFB of concrete slabs mounted internally, subjected to cased and uncased charges, received from Mr. Tim Knight at the US Army Corps of Engineers Omaha District, December 1993.

Figure 1. Spall and Breach Data Scaled After McVay

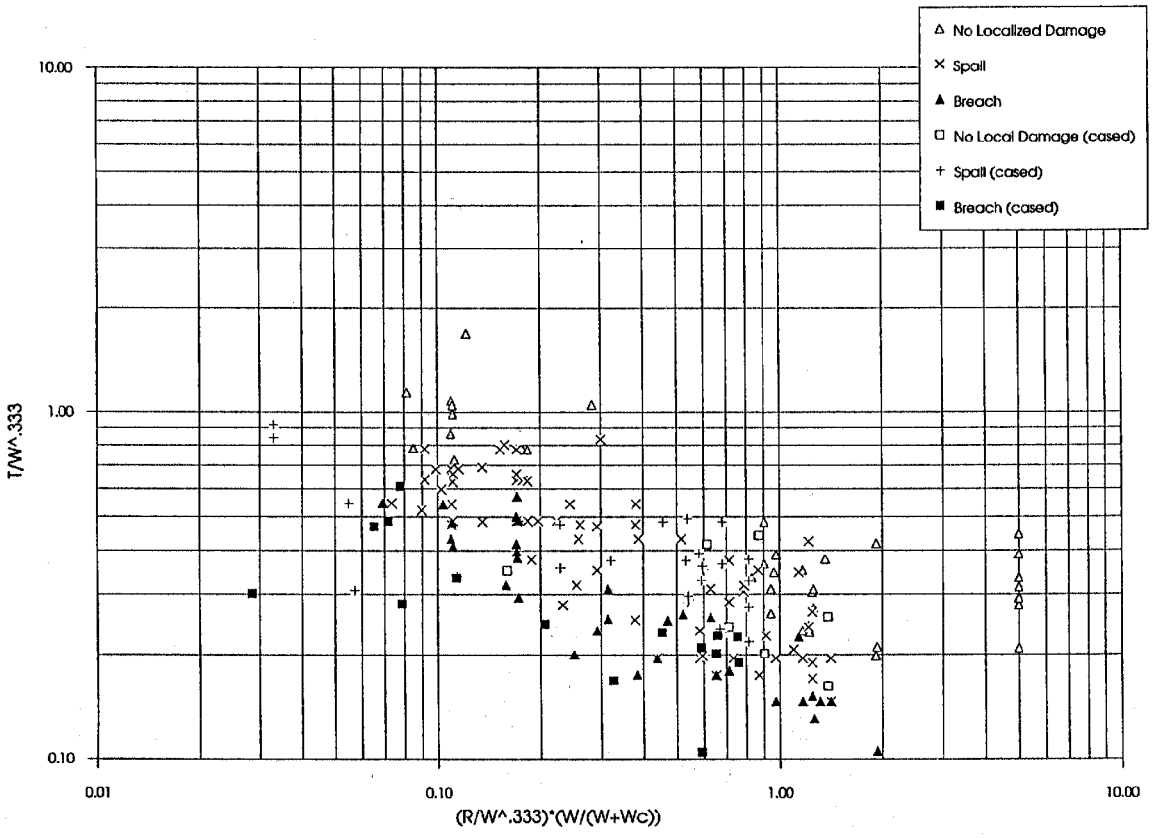

Figure 1. Spall and Breach Data Scaled After McVay

Figure 2. Spaii Data Scaled According to ARA 5555

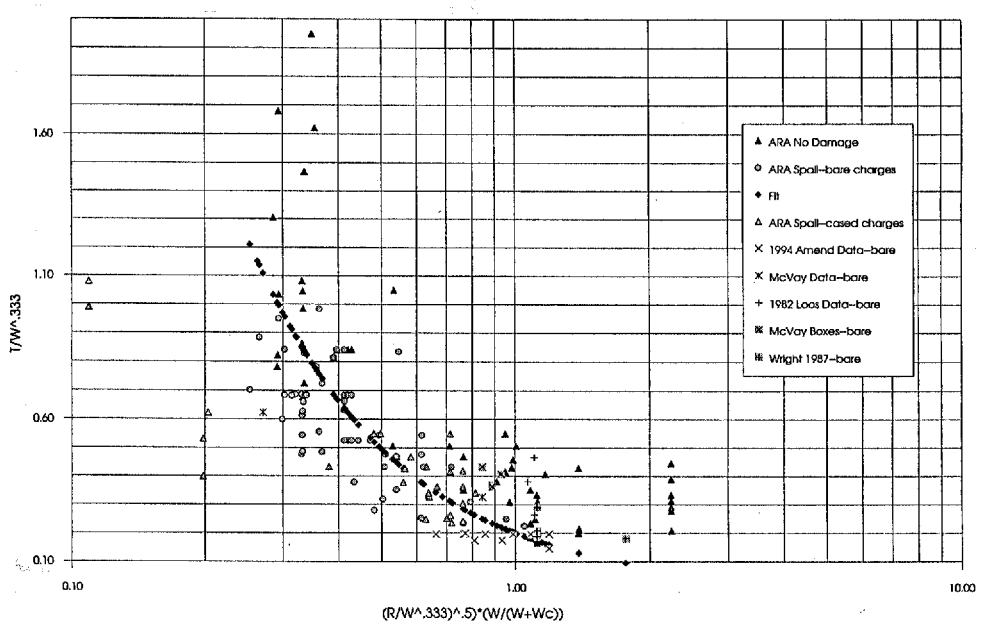

Figure 2. Spall Data Scaled According to ARA 5555

Figure 3. Spall and Breach Data, Scaled R after McVay, Scaled T as T/R

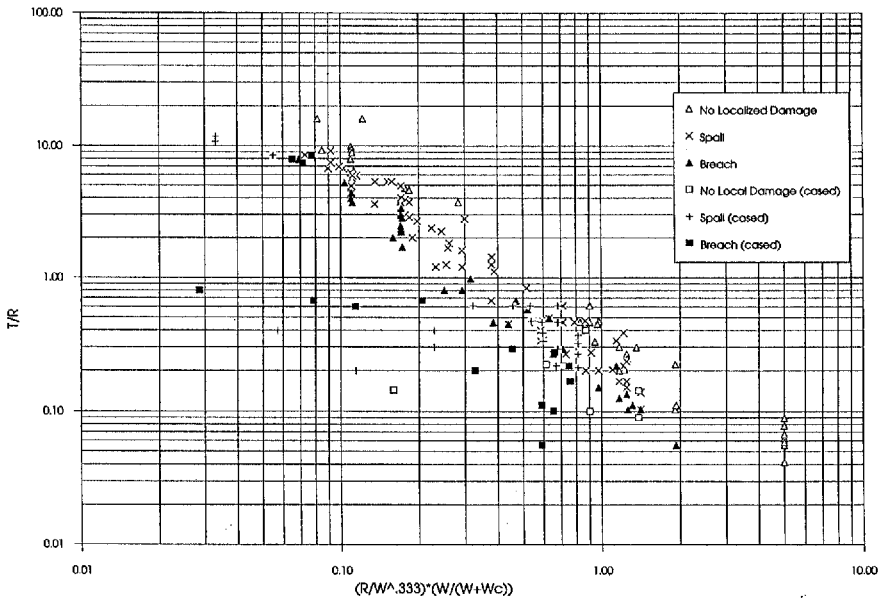

Figure 3. Spall and Breach Data, Scaled R after McVay, Scaled T as T/R

Figure 4. Spaii and Breach Data, Scaled R as McVay with Case

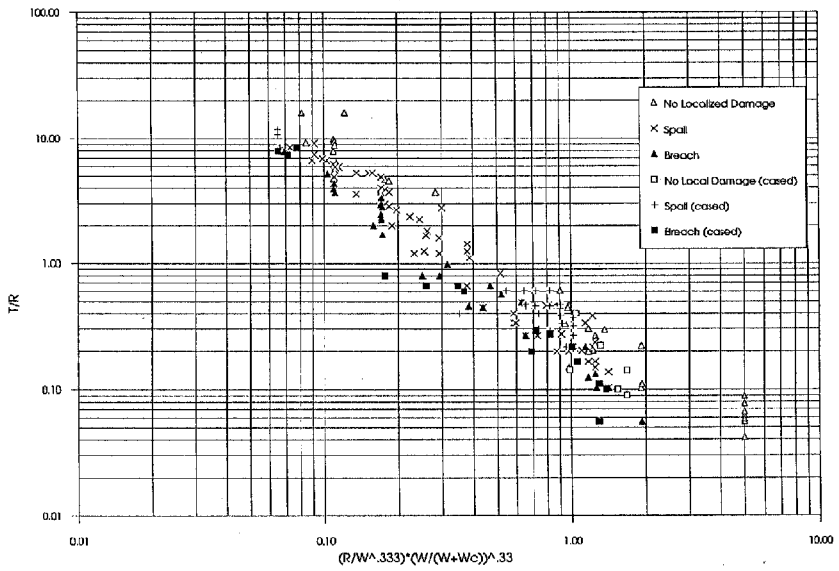

Figure 4. Spall and Breach Data, Scaled R as McVay with Case Factor Adj., Scaled T as T/R

Figure 5. Spall and Breach Data Scaled for Strength (Rate Effects), Case Thickness and Aspect Ratio

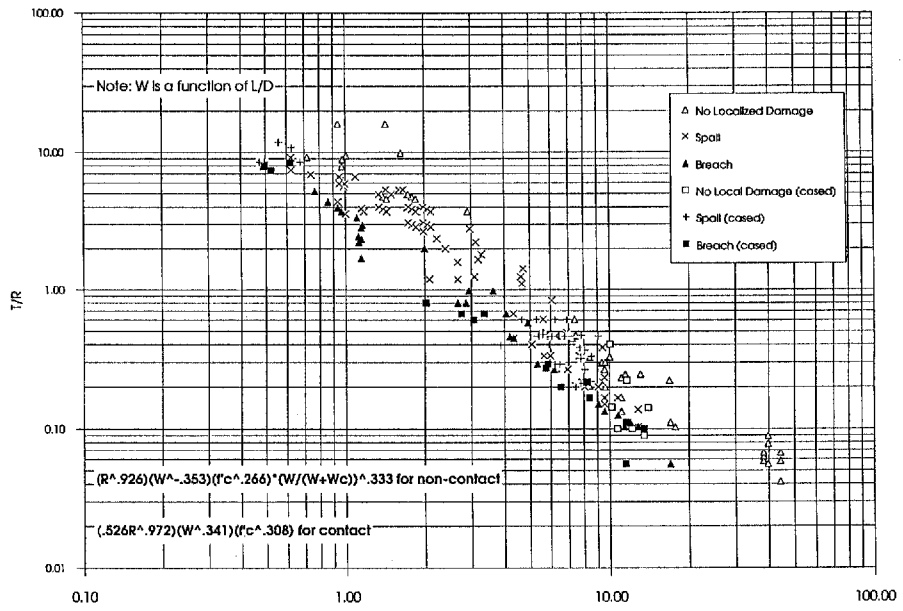

Figure 5. Spall and Breach Data Scaled for Strength (Rate Effects), Case Thickness and Aspect Ratio

Figure 6. Spail and Breach Data Scaled for Strength (Rate Effects), Case Thickness and Aspect Ratio (Full Range)

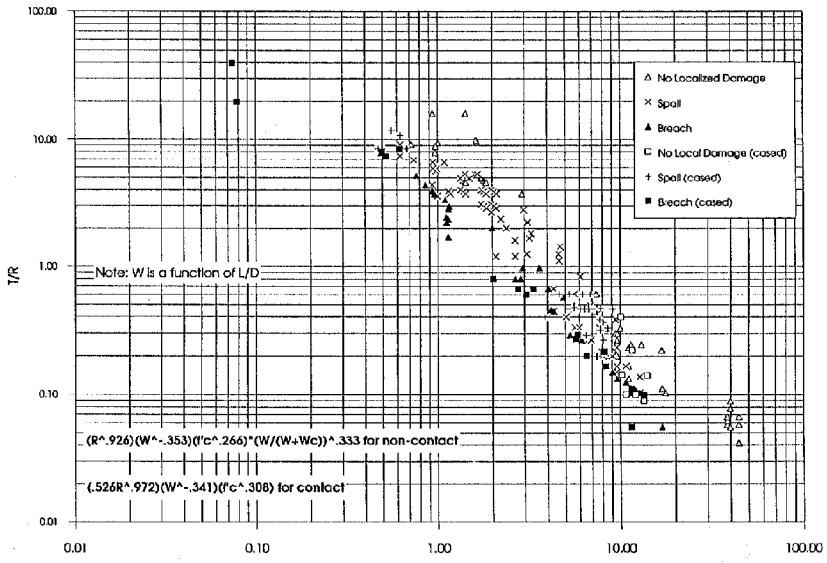

Figure 6. Spall and Breach Data Scaled for Strength (Rate Effects), Case Thickness and Aspect Ratio (Full Range)

Figure 7. Spall and Breach Prediction Including Aspect Ratio and Strength with Rate Effects

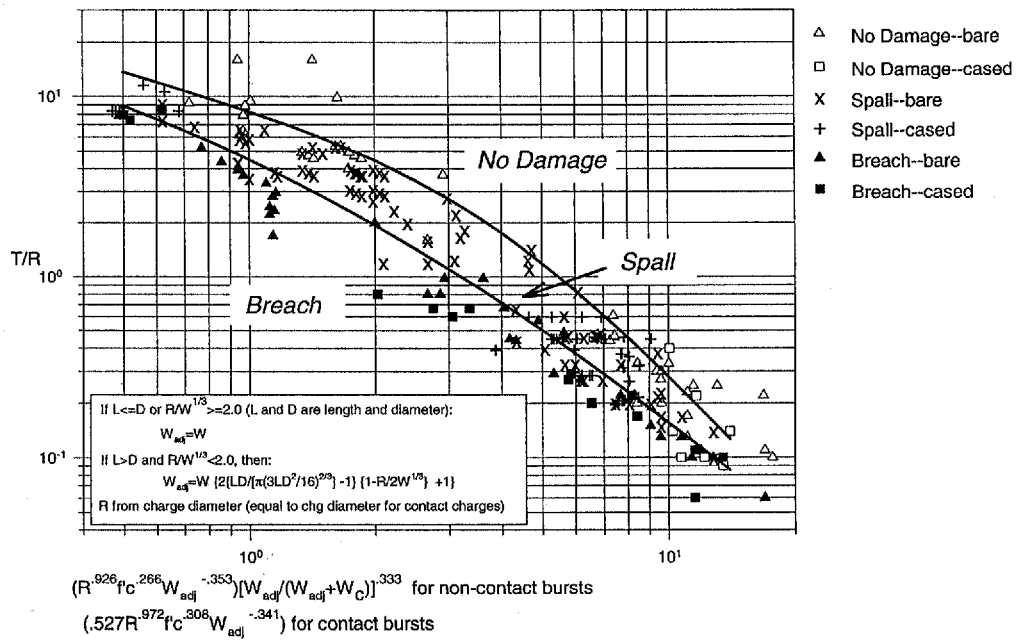

Figure 7. Spall and Breach Prediction Including Aspect Ratio and Strength with Rate Effects

Figure 8. Spail and Breach Prediction Including Aspect Ratio and Strength with Rate Effects--95% Prediction for Spail Data (All Data Shown)

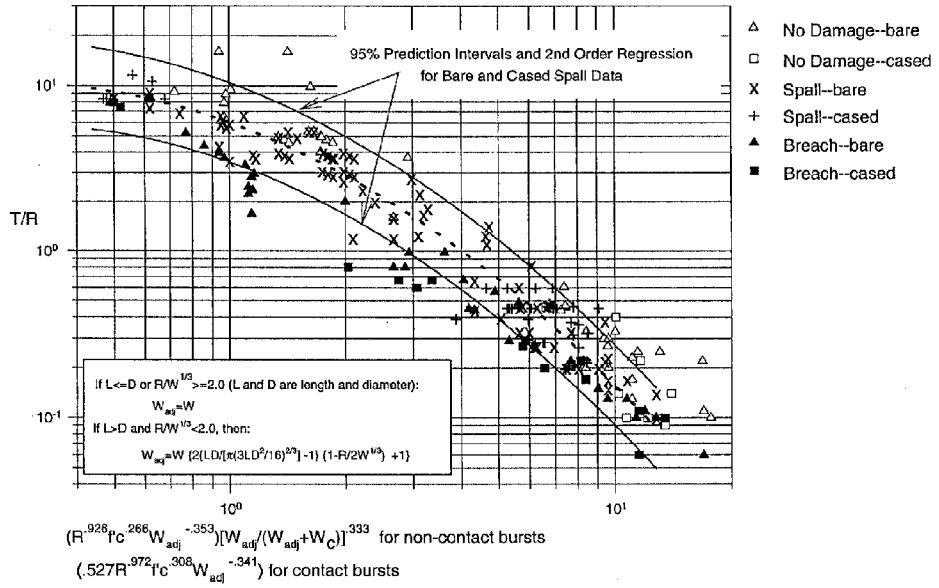

Figure 8. Spall and Breach Prediction Including Aspect Ratio and Strength with Rate Effects--95% Prediction for Spall Data (All Data Shown)

Figure 9. Spall and Breach Prediction Including Aspect Ratio and Strength with Rate Effects--95% Prediction for Spall Data (Spall Data Only Shown)

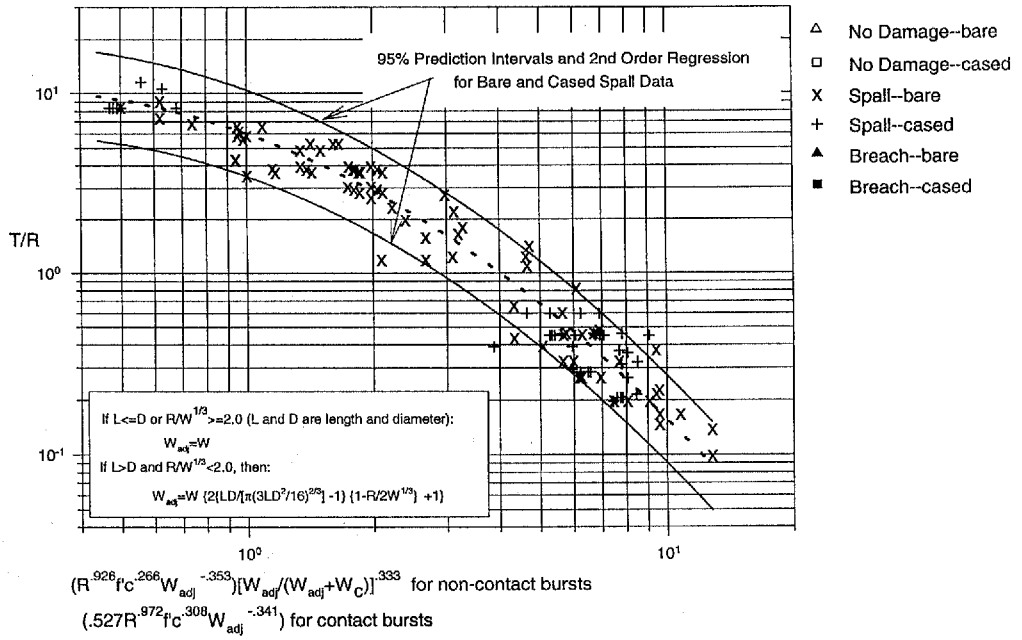

Figure 9. Spall and Breach Prediction Including Aspect Ratio and Strength with Rate Effects--95% Prediction for Spall Data (Spall Data Only Shown)

Figure 10.
Spall and Breach Data Comparisons--Effects of Experiment Scale

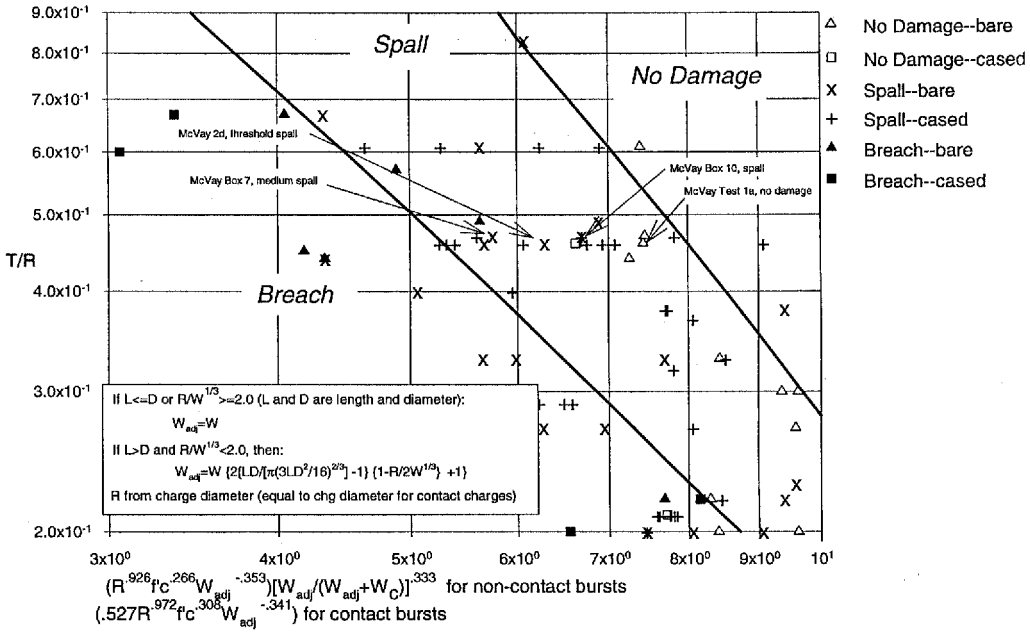

Figure 10. Spall and Breach Data Comparisons--Effects of Experiment Scale

Figure 11. Spall and Breach Data Comparisons--Casing Effects at Larger Standoffs

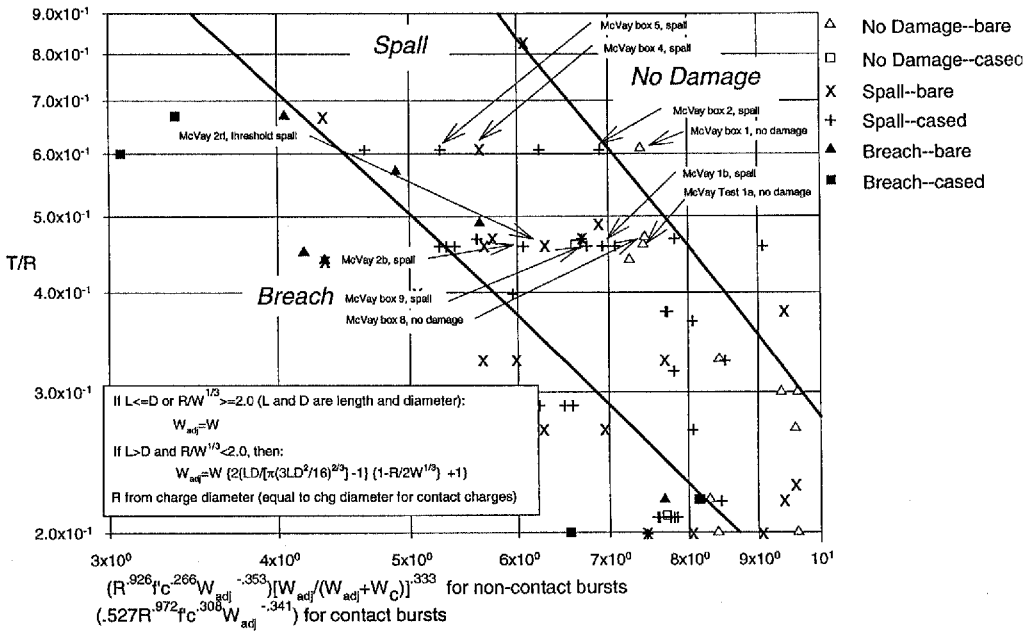

Figure 11. Spall and Breach Data Comparisons--Casing Effects at Larger Standoffs

Figure 12.
Spall and Breach Data Comparisons--Casing Effects at Smaller Standoffs

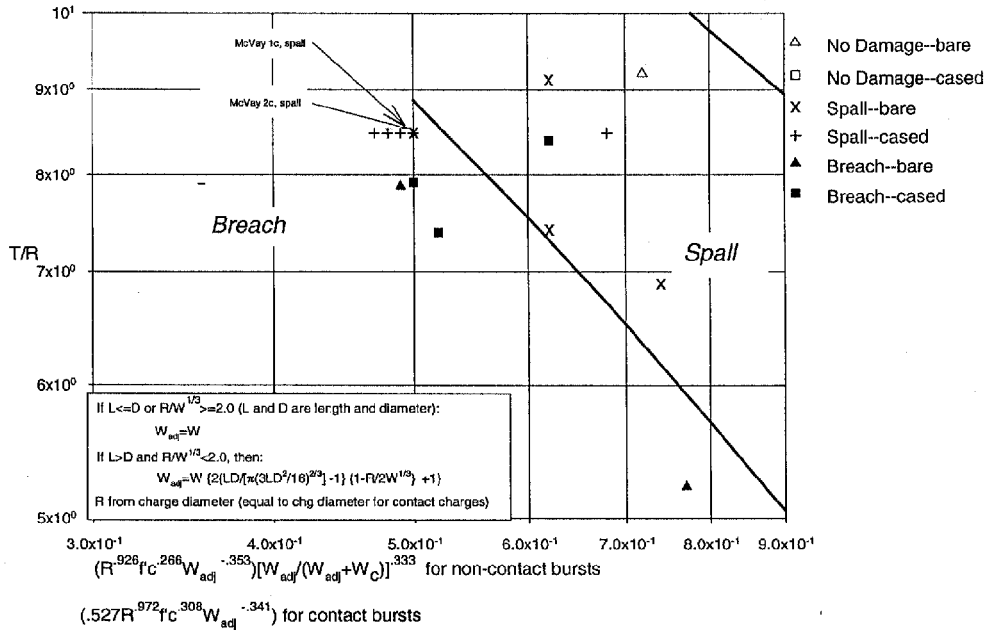

Figure 12. Spall and Breach Data Comparisons--Casing Effects at Smaller Standoffs

Figure 13. Spall and Breach Data Comparisons--Effects of Charge Shape

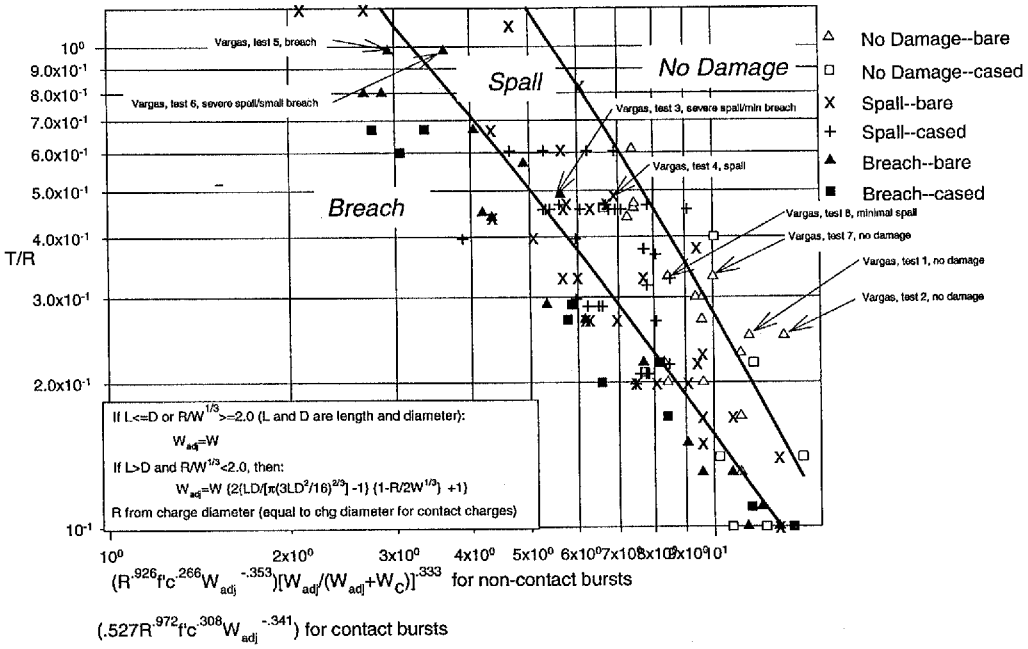

Figure 13. Spall and Breach Data Comparisons--Effects of Charge Shape